

Article

# Separation of Products from Mineral Sequestration of CO<sub>2</sub> with Primary and Secondary Raw Materials

Dario Kremer \*  and Hermann Wotruba

AMR Unit of Mineral Processing, RWTH Aachen University, 52064 Aachen, Germany;  
wotruba@amr.rwth-aachen.de

\* Correspondence: kremer@amr.rwth-aachen.de

Received: 17 November 2020; Accepted: 4 December 2020; Published: 7 December 2020



**Abstract:** Rising levels of greenhouse gases (GHG) in our atmosphere make it necessary to find pathways to reduce the amount of GHG, especially emissions of CO<sub>2</sub>. One approach is carbon capture and utilization by mineralization (CCUM). With this technology, it is possible to bind CO<sub>2</sub> chemically from exhaust gas streams in magnesium or calcium silicates. Stable products of this exothermic reaction are carbonates and amorphous silica. Being amongst the biggest emitters of CO<sub>2</sub>, the cement industry has to find ways to reduce emissions. Geological mapping in Europe has been carried out to find suitable feedstock material, mainly olivines but also slags, to perform lab-scale carbonation tests. These tests, conducted in a 1.5 L autoclave with increased pressure and temperature, have been scaled up to a 10 L and a 1000 L autoclave. The outcomes of the carbonation are unreacted feed material, carbonate, and amorphous silica, which have to be separated to produce substitutes for the cement industry as pozzolanic material (amorphous silica) or a value-added product for other applications like paper or plastics (magnesite/calcite with bound anthropogenic CO<sub>2</sub>). Therefore, a process for the separation of ultrafine carbonation product was developed, consisting mainly of classification and flotation.

**Keywords:** carbon capture and utilization; mineral sequestration of CO<sub>2</sub>; mineral processing; global warming; carbon dioxide; olivine

## 1. Introduction

The emissions of GHG into our atmosphere, especially carbon dioxide are increasing rapidly. In 2019, global carbon dioxide concentration was 409.8 ppm with an annual increase of 2.4 ppm from 2018, whereas in the 1960s the increase of CO<sub>2</sub> emissions was about 0.6 ppm per year [1,2].

This fact leads to research efforts in the field of reduction of CO<sub>2</sub> emissions by means of storing or utilization. One approach is carbon capture and utilization by mineralization (CCUM), an accelerated carbonation process with increased temperature and pressure. Carbon dioxide reacts with calcium and magnesium oxide in an exothermic reaction forming stable carbonates [3]. Natural raw materials for this reaction could be ores with a high content of magnesium or calcium silicates such as serpentinite, peridotite, wollastonite and also secondary materials like fly ashes and metallurgical slags [4–6]. For simplicity, the primary input material for the process is named olivine in the following study, although it is a peridotite with ~80 wt.% olivine content [7].

The CO<sub>2</sub>MIN project investigates the process of chemically binding carbon dioxide (see Formula (1)) from flue gas emissions in primary and secondary raw materials with the objective of generating a value-added additive for the production of building materials. Therefore, suitable feed material is pretreated and carbonated in a pressurized reactor, followed by separation of the reaction products to generate a marketable product. The main focus of this study is the development of a separation process for the carbonation products. The interdisciplinary consortium of the CO<sub>2</sub>MIN project

consists of HeidelbergCement AG (coordination, analyses, application tests), RWTH Aachen University with five departments (analysis of potential feedstock, sample preparation, carbonation process, process modelling, analyses, separation of products, Life Cycle Assessment) and the Potsdam Institute for Advanced Sustainability Studies (IASS Potsdam) (analysis of economic factors and social acceptance), supported by the Dutch start-up Green Minerals (consulting) [6,8].

The process flowsheet (Figure 1) shows lab-scale carbonation tests (1.5 L and 10 L) as well as upscaling test work in a 1000 L autoclave to transfer the gained knowledge into more application-oriented procedures with higher throughputs and to receive sufficient carbonated product for application tests as substitute material for cement and as filler in paper and rubber.

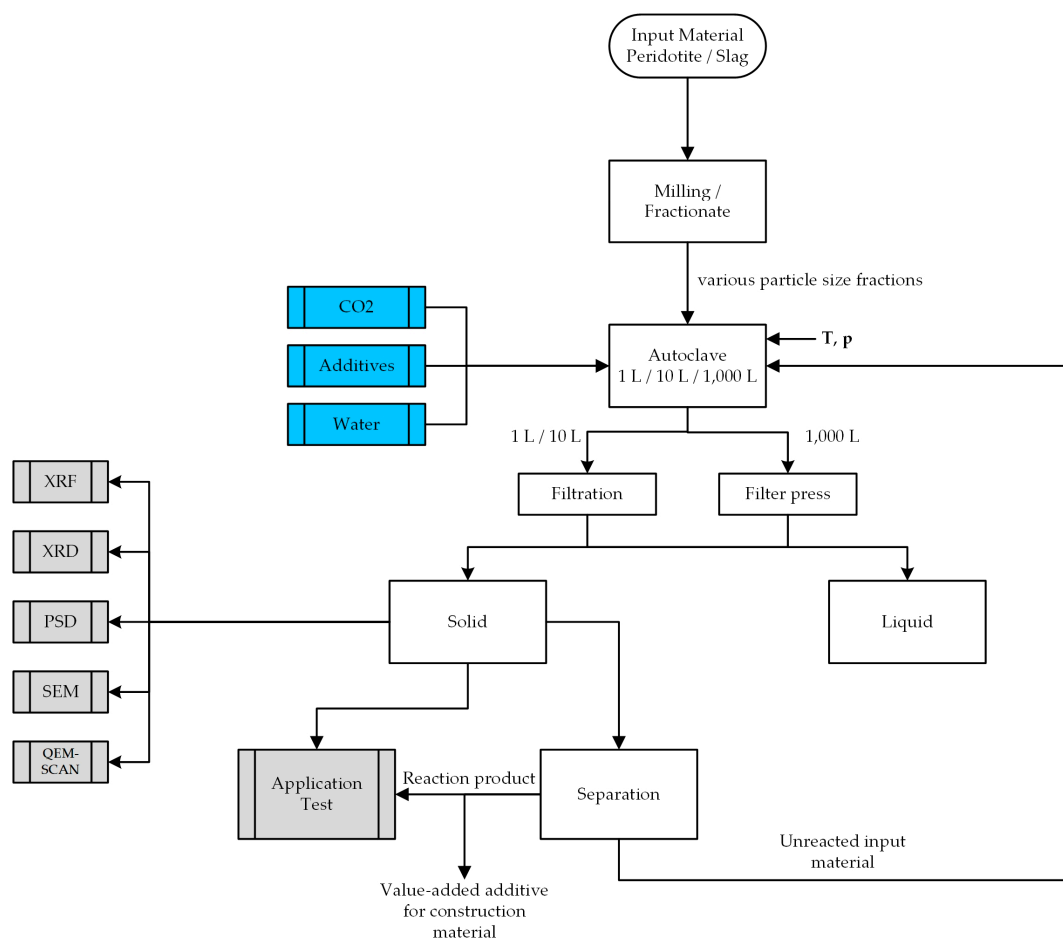
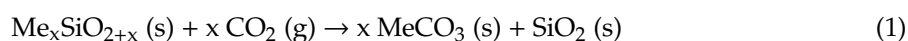


**Figure 1.** CO2MIN flowsheet of carbonation with associated processes. (PSD—particle size distribution).

The exothermic reaction (Formula 1) shows the sequestration of carbon dioxide [9,10].



The input material must contain magnesium or calcium silicate to bind the carbon dioxide. Products of the sum of partial reactions are amorphous silica and magnesite—respectively calcite—in which the CO<sub>2</sub> is bound stable since it possesses the lowest free energy of formation in comparison to other carbon compounds [5]. In the CO2MIN project, olivines from different deposits in Europe have been used with contents of 55–80% forsterite as magnesium silicate, which reacts with the carbon dioxide. The reaction naturally takes place in geological periods, but can be accelerated by increasing temperature and pressure, which is done in an autoclave, but also with suitable pretreatment by increasing the particle surface.

Due to its pozzolanic properties, the amorphous silica could serve as clinker replacement material, significantly decreasing anthropogenic CO<sub>2</sub> emissions, as ~500 kg CO<sub>2</sub> are emitted for each ton of cement clinker produced [11,12]. Further applications are, amongst others, refractory materials and deoxidizers in steel making ceramic matrix composites [13]. Magnesite and calcite can be used as a filler, e.g., in the production of synthetic rubber [14,15]. The focus of the following paper is the carbonation of olivine with focus on the product separation, but the results for secondary raw materials as slags are also described.

## 2. Materials and Methods

### 2.1. Examination of Possible Input Material

Possible feedstock for the carbonation process are alkaline earth metal oxides that occur but are not limited to minerals like olivine ( $Mg_{1.6}Fe_{2+0.4}(SiO_4)$ ), serpentine ( $Mg_3Si_2O_5(OH)_4$ ) and wollastonite ( $CaSiO_3$ ), as well as steel slag and fly ash [16–20]. The main subjects of the investigation for CO<sub>2</sub>MIN project are olivines with mainly forsterite as reactive component. Basalt from Germany, olivine from Japan and steel slag, fly ash and red mud from European deposits have also been investigated. The investigated deposits for basalts and ultramafic rocks are shown in Figure 2. Olivine-bearing rocks occur in several different geological settings throughout Europe. The big deposits are normally part of ophiolite complexes and ultramafic intrusions like the largest deposit in Norway, the Almklovdaalen peridotite massif, where Steinsvik Olivine AS is producing [7].

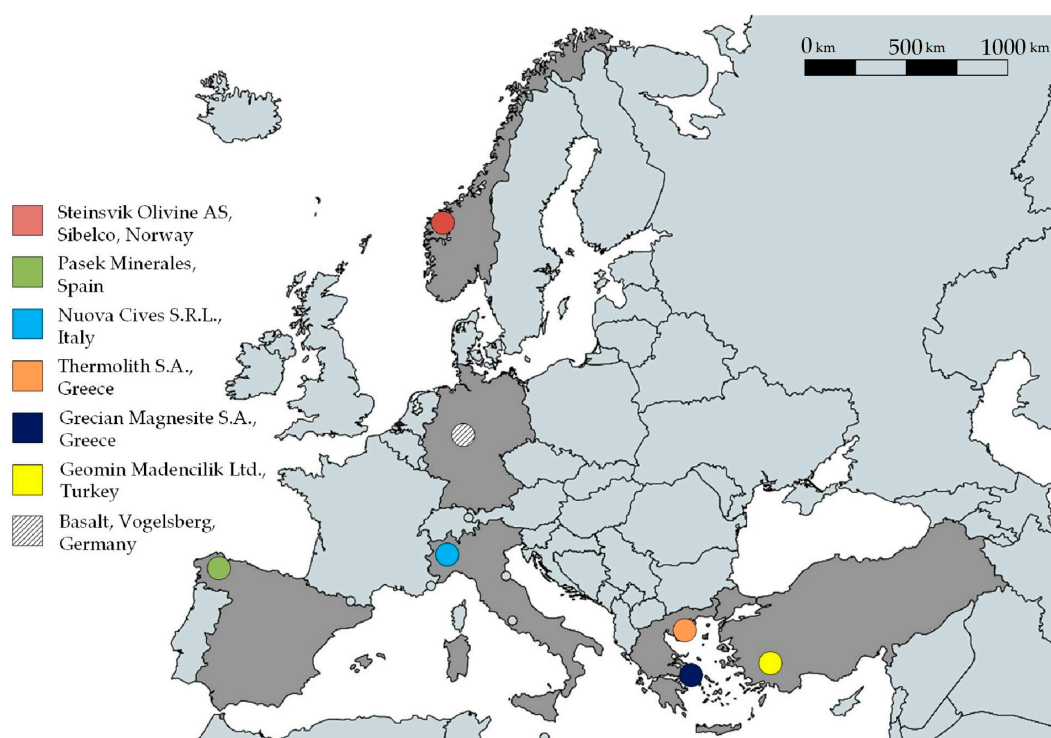


**Figure 2.** Origin and producer of samples tested for the use in the carbonation process [7].

Samples of the highlighted deposits were analyzed via XRF, XRD, LOI, partly QEMSCAN, and SEM and assessed in terms of potential for the carbonation process.

Elemental composition was determined by X-ray fluorescence (XRF) technique using a PW2404 device by Malvern PANalytical B.V. (Eindhoven, Netherlands). X-ray diffraction (XRD) method was applied using a Bruker D8 Advance device in Bragg–Brentano geometry by Bruker AXS (Karlsruhe, Germany), equipped with LynxEye detector, CuK $\alpha$  tube and nickel filter. The chosen XRD parameters included a measurement range from 5–90° 2 $\theta$  in 0.02° steps at 2s per step. To enable a

comparison of the present mineral phases as indicated by the components detected via XRF technique, XRD analysis was combined with semiquantitative evaluation of the mineral phase fractions. As this study focusses on natural resources, which are subject to fluctuations, this semiquantitative approach is considered sufficient for the aimed comparison. [7] A quantitative QEMSCAN analysis of different olivines has been performed previously by Kremer et al. [7] by applying a Quanta 650-F QEMSCAN (FEI/Thermo Fischer, Hillsboro, OR, USA) scanning electron microscope (SEM). The measurements were conducted with an acceleration voltage of 25 kV and a fixed sample current of 10 nA. The surface of each sample section was scanned with a spatial resolution of 5  $\mu\text{m}$ . Back scatter (BSE) intensities and individual X-ray spectra were recorded for each pixel with a 4-quadrant BSE detector and two DualXFlash 5030 SDD (Bruker AXS, Karlsruhe, Germany) energy dispersive x-ray spectrometers (EDX). SEM analysis was performed with a ZEISS GeminiSEM500 (Carl Zeiss AG, Oberkochen, Germany).

With the investigated European olivine deposits plus the Horoman Mine in Japan, which was also analyzed, CO2MIN covers over 50% of the annual global olivine production of between 7800 and 9000 ktpa [7,21].

The mineralogical and chemical composition of the investigated samples showed similar results. The olivines mainly consisted of forsterite (55–80%) and enstatite (10–30%) with small amounts of lizardite ( $\leq 5\%$ ). In one sample 10–15% tremolite was detected. Besides 10–15% forsterite, basalt mainly consisted of albite, anorthite and quartz. XRF analysis of one olivine sample (Table 1) showed high SiO<sub>2</sub> and MgO contents and minor amounts of other oxides like Fe<sub>2</sub>O<sub>3</sub>, Al<sub>2</sub>O<sub>3</sub>, NiO and CaO. Basalt had lower contents of MgO (9%), but higher contents of CaO with 9.8% [7].

**Table 1.** XRF analyses of the feed material for the carbonation.

Component [wt.%]	Olivine	Ferrochrome Slag
	Norway	Germany
SiO <sub>2</sub>	48.6	32.7
Al <sub>2</sub> O <sub>3</sub>	0.5	6.3
Fe <sub>2</sub> O <sub>3</sub>	7.8	0.2
TiO <sub>2</sub>	0.0	0.2
CaO	0.2	43.9
MgO	41.1	11.6
K <sub>2</sub> O	0.1	0.1
Na <sub>2</sub> O	0.0	0.0
NiO	1.2	0.0
Cr <sub>2</sub> O <sub>3</sub>	0.4	4.7

According to analyses, availability and results from the carbonation tests it was decided to use the olivine from Steinsvik Olivine AS for further investigations, which are part of the following description [7,22].

As secondary feed material for the carbonation process different slags, fly ashes and red mud have been investigated for their potential binding of CO<sub>2</sub>. These secondary materials are far more heterogeneous in composition than primary feed material, mainly consisting of calcium, magnesium and iron silicates and oxides, namely merwinite, bredigite, monticellite, akermanite, wuestite, larnite, mayenite and spinel. According to analyses, availability and results from the carbonation tests, it was decided to use a ferrochrome slag from Germany for further large-scale carbonation experiments and for separation tests. The elemental composition of this slag is listed in Table 1 with high amounts of CaO and SiO<sub>2</sub> and minor contents of MgO, Al<sub>2</sub>O<sub>3</sub> and Cr<sub>2</sub>O<sub>3</sub>.

## 2.2. Pretreatment

Pretreatment of the feed material is necessary to enhance reactivity by increasing the reactive surface through grinding and milling. The milling and classification of the feedstock material for the lab-scale carbonation tests in 1.5 L and 10 L autoclave were performed in the technical laboratory of

the Unit of Mineral Processing (AMR) of RWTH Aachen University with a roller mill (Type LWBP 2/2, Karl Merz Maschinenfabrik GmbH, Heschingen, Germany) and screens (Prüf 86, Siebtechnik GmbH, Mühlheim an der Ruhr, Germany) to obtain the three particle size fractions 100–200  $\mu\text{m}$ , 63–100  $\mu\text{m}$  and 20–63  $\mu\text{m}$ . The fraction <20  $\mu\text{m}$  was obtained by milling in a planetary ball mill (PM 4, Retsch GmbH, Haan, Germany) followed by wet screening. Feedstock for large-scale carbonation tests in a 1000 L autoclave was milled with a vertical roller mill (LM3, 6/4, Loesche GmbH, Düsseldorf, Germany) followed by direct classification within the milling chamber by an air classifier (LSKS 6, Loesche GmbH, Düsseldorf, Germany). For the large-scale carbonation tests of the olivine only the fractions 0–20  $\mu\text{m}$  and 0–63  $\mu\text{m}$  were prepared and the slag was milled below 63  $\mu\text{m}$ .

### 2.3. Lab-Scale Carbonation

The first carbonation tests were performed in a 1.5 L autoclave (Type 3E Büchi Kiloclave, Büchi AG, Uster, Switzerland). The carbonation process was first tested with a reference material, a high-grade dead burned magnesia with 97.56 wt.% MgO. The results, visible in the XRD pattern [23], showed a complete conversion of the periclase to magnesite which underlined the effectiveness of the process for the selected parameters regarding pressure, temperature, particle size and stirring speed (see Section 2.4). Carbonation tests were performed in this autoclave for all investigated samples (see Figure 2). Olivine from Steinsvik Olivine AS has been used for further test work to find best parameters for maximum CO<sub>2</sub> uptake. More experiments with the specified parameters were performed with a 10 L autoclave, which resulted in larger product volumes for the first separation tests. As the next step, experiments were up-scaled to a 1000 L reactor, which was necessary to generate sufficient amounts of carbonated product in order to perform application tests to determine the potential suitability as a clinker substitute and further separation tests on larger scale. The carbonation products of the 1.5 L and 10 L autoclave products were filtered by vacuum filtration and the large-scale products were filtered with a filter press. The liquid fraction was analyzed via ICP-OES, while the solid fraction was also analyzed. The solid products of the large-scale carbonation tests of olivine and slag were split into two samples each. One sample was directly used for application tests and the other one was further processed to separate the unreacted input material from magnesite, respectively calcite, and amorphous silica.

### 2.4. Experimental Conditions and Procedures

Numerous experiments have been carried out to determine the process conditions for maximum carbonation degree. Stopic et al. [23,24] conducted research on temperature, pressure, stirring speed, retention time, additives and solid liquid ratio based on literature data to determine standard experimental parameters for the carbonation [25,26].

The research on experimental parameters for the carbonation reaction in the 1.5 L and 10 L autoclaves resulted in the following process conditions for the large-scale test work (Table 2).

**Table 2.** Process conditions for 1000 L autoclave carbonation tests.

Experimental Parameters	
Temperature:	175 °C
Pressure:	$p_0 = 17.5 \text{ bar}$ , $p_{\text{max}} = 30 \text{ bar}$ (limitation of 1000 L autoclave)
Stirring Speed:	600 rpm
Retention Time:	4 h
Solid/Liquid Ratio:	1:8
Additives:	0.64 M sodium bicarbonate 0.05 M oxalic acid 0.01 M ascorbic acid

### 2.5. Separation of Carbonation Products

Previous studies showed different specific particle sizes for the reaction products magnesite (<25  $\mu\text{m}$ ) and amorphous silica (~20 nm) [27,28]. Figure 3 shows SEM pictures of the carbonation products of olivine from Aheim Gusdal pit in different feed particle size fractions with particle sizes of 3–5  $\mu\text{m}$  for magnesite and around 100–200 nm for amorphous silica.

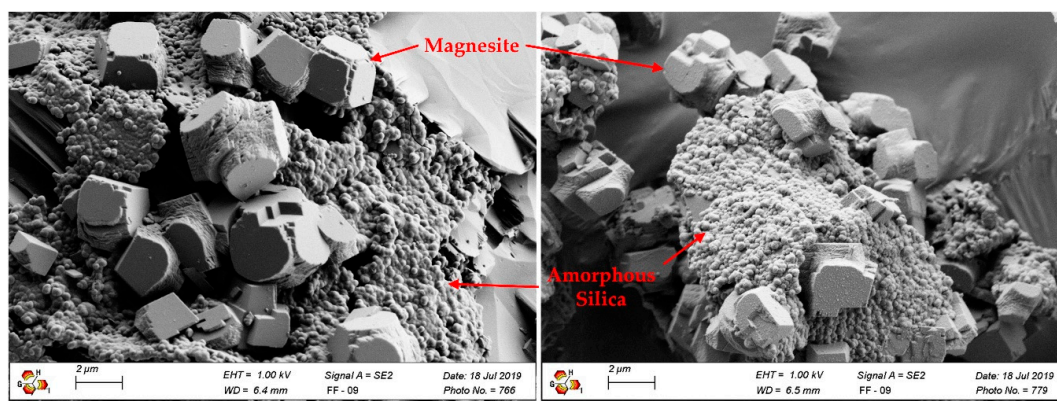


**Figure 3.** SEM images of reaction products of Norwegian feedstock material, magnified 5000 $\times$ . Initial particle size 20–63  $\mu\text{m}$  (left picture) and 0–20  $\mu\text{m}$  (right picture).

The reaction products magnesite and amorphous silica have the same particle size regardless of the particle size of the feed material (Figure 3). The recovery of nickel, magnesium and iron from the product during leaching with hydrochloric acid has been studied by Matus et al. [29].

Based on this differing particle size of the reaction products and the different hydrophobic and surface properties, the following options for separation are examined in the CO<sub>2</sub>MIN project:

Separation by flocculation: selective flocculation of the (magnesium-) carbonates with fatty acids and separation of the flocculated agglomerates by classification (e.g., up-current-classifier).

Separation by flotation: unreacted silicates might be separated by flotation with amines as collectors. Another option could be the classification of the product prior to flotation to separate magnesite and microsilica from coarse unreacted olivine. In the next step, magnesite can be separated in the foam product with fatty acids as collectors. A problem might be the fine particle size of the magnesite. To determine the reagents regime, limits of particle size, pH value and other parameters, monomineral flotation has been tested for single phase olivine, magnesite and amorphous microsilica. This resulted in further investigations with artificial mixtures of the different phases, followed by flotation of carbonation products.

Separation by classification: The reaction products agglomerate or precipitate on the olivine particles, but do not interact with each other [30]. Particle liberation is necessary to provide successful separation tests. Therefore, different options for de-agglomeration have been tested, namely attrition with or without dispersant (sodium silicate), ultrasonic treatment (UP400St, Hielscher Ultrasound Technology, Teltow, Germany) with a frequency of 24 kHz, 10 g of sample in 1 L water and a retention time of 5–20 min, as well as further comminution with mortar mill and disc mill. Agglomeration could be a consequence of drying prior to SEM analysis or precipitation kinetics. The unreacted olivine is present in the particle size range of the respective feed material. The separation of the unreacted material from the reaction products was tested. Tests have been performed at lab-scale with fine sieves (5  $\mu\text{m}$ , 11  $\mu\text{m}$ , 15  $\mu\text{m}$ , 20  $\mu\text{m}$ ). For higher throughput other options have to be tested, e.g., a 10 mm hydrocyclone or a classification centrifuge.

### 3. Results

#### 3.1. Results of Flocculation

Flocculation of magnesite from the carbonation product was examined in a stirring tank with a volume of 300 mL and a solid liquid ratio (s/L) of 1:30 with addition of oleic acid (200–700 g/t) and retention time of 10 min, followed by classification in an up-current classifier. Another approach was the coating of polyethylene beads with oleic acid and addition into the stirring tank to agglomerate with the magnesite and serve as a carrier for the carbonates, followed by separation of the coated beads from the tank and subsequent rinsing of the carbonates from the beads.

This treatment lead to a visible agglomeration in the tank, which was not selective, as the following analysis revealed. The flocculation product contained magnesite, amorphous silica and unreacted olivine, hence no separation was detectable. An issue of the usage of fatty acids is the limited selectivity, as all available carbonates interact with this flocculant. Fatty acids produce insoluble complexes with all divalent cations in solution and hydrophobicize them [31].

#### 3.2. Results of Flotation

Flotation tests were conducted for the carbonated olivines. The carbonation product to be processed contained 65–75% unreacted material, 20–25% magnesite and 5–10% amorphous silica, which was stoichiometrically calculated by the ratio to the reaction product magnesite (Table 3).

Therefore, the separation of the unreacted olivine is an important step, also with regards to circulation of this mass flow back to the carbonation reactor. The flotation scheme consisted of monomineral flotation of olivine, magnesite and microsilica to determine the floatability of the single minerals, followed by flotation of an artificial mixture of magnesite and microsilica, which resulted in the final step of flotation of the actual carbonation product.

The flotation of the unreacted olivine was tested as a first flotation step, which was simulated by flotation of raw input material, the pure Norwegian olivine <20 µm with dodecylamine as collector, MIBC as frother and at neutral pH. This flotation test resulted in a recovery of up to 94.5%. To determine the effect of dodecylamine on the reaction products magnesite and amorphous silica, monomineral flotation tests for these two minerals have also been carried out. Magnesite and silica were not affected by the collector and stayed in the hydrophilic fraction during monomineral flotation with dodecylamine.

**Table 3.** Semiquantitative XRD examination of the present mineral phase fractions in Norwegian olivine before and after carbonation and one flotation product. Amorphous silica was determined arithmetically by stoichiometry.

Mineral Phase Fraction [%]	Olivine (Steinsvik)		
	Input Material	Carbonation Product	Flotation Product
Forsterite	75–80	50–55	45–50
Enstatite	10–15	10–15	5–10
Lizardite	≤5	≤5	≤5
Clinochlore	≤5	≤5	≤5
Talc	≤5	≤5	≤5
Magnesite	-	20–25	30–35
Amorphous Silica	-	5–10	indeterminable

As a next step, the monomineral flotation of magnesite with fatty acids as collector was tested in different concentrations resulting in a recovery of >90% for the fraction 20–63 µm, demonstrating the applicability for magnesite separation in general and providing results for the reagents regime for further examinations. Amorphous silica is not affected by the collector. Highest recovery was obtained by using oleic acid as collector, MIBC as frother and no depressant. Reducing the particle size of magnesite to below 20 µm resulted in a significant drop in recovery to 16%. Yao et al. recommended

an increase in pH value for the flotation of magnesite. The experiments with a pH value of 12 enhanced the recovery for magnesite <20  $\mu\text{m}$  to ~90% [32].

Subsequently, artificial mixtures for simulation of the reaction products without unreacted material—consisting of 65% magnesite and 35% microsilica—were part of flotation test work. The best results were achieved for oleic acid without depressor at pH 12 with a recovery of 76% MgO in flotation product (~88% in used magnesite) at a purity of >75%.

As final test, a flotation experiment with the previous results was conducted for the actual carbonated product and can be seen in Table 3, resulting in an increase of magnesite of 10% to 30–35%, which meant a recovery of 72.2% at a yield of 50%.

Further flotation investigations (monomineral flotation at particle sizes below 5  $\mu\text{m}$ , the effect of stirring speed, agitation and flotation time) and the combination of different processes (classification prior to flotation) are part of current research.

### 3.3. Results of Deagglomeration and Classification

The separation tests for the carbonated material via flocculation have not been successful. The results of flotation are promising, but SEM images still showed a silica layer and some magnesite particles on the surfaces of the unreacted olivine. Therefore, it was decided to firstly set the focus on deagglomeration. It seems that the magnesite and the amorphous silica do not precipitate on the surface of the olivine but grow on the surface with a strong bond. Consequently, deagglomeration was investigated by means of ultrasonic treatment in different intensities, attrition with or without dispersant and varying s/L ratio and retention time as well as further comminution. Comminution with mortar mill or disc mill showed good results under SEM regarding liberation but lead to negative side effects by reducing the particle size of the unreacted olivine particles. Ultrasonic treatment and attrition were conducted in liquid medium, followed by screening to classify the liberated particles before drying, which is necessary for the analysis. Both deagglomeration options showed similar results and usage of dispersant had no positive effect. Concerning availability and higher throughput attrition was used for deagglomeration before the following separation tests. A higher retention time ensured better separation. After evaluating the results, the parameters of the attrition were set to 25–30% water content and stirring speed of 1100 rpm for 240 min to deagglomerate the carbonation products.

As the amorphous silica content cannot be analyzed directly, the magnesite serves as an indicator for successful deagglomeration. In Figure 4, the XRD pattern for fraction 11–20  $\mu\text{m}$  is shown before and after attrition. Before attrition, magnesite could be found in the product sample. After attrition, no more magnesite peaks were visible in the XRD spectrum, which stated a successful liberation.

Further attrition and classification tests were conducted for both the olivine and the ferrochrome slag carbonation products to evaluate the successful separation via classification. Therefore, narrow particle size fractions of the carbonation products were produced by sieving. The XRD patterns for the olivine carbonation products can be found in Figure 5.

It is evident that the magnesite peaks are the highest in the 0–5  $\mu\text{m}$  fraction with less enstatite and chlinochlore peaks, whereas in the fraction 11–15  $\mu\text{m}$  there is only one small peak for magnesite. This qualitative statement can be confirmed with Table 4, which gives a semiquantitative determination of the contained minerals phases.

The fraction 0–5  $\mu\text{m}$ , which—based on an optimal attrition—is supposed to contain the whole magnesite (2–5  $\mu\text{m}$ ) and amorphous silica (100–200 nm) shows an increased amount of magnesite of 30–35%, which means a recovery of 65% at a yield of 45%. In the other particle size fractions, the amount of magnesite was reduced.

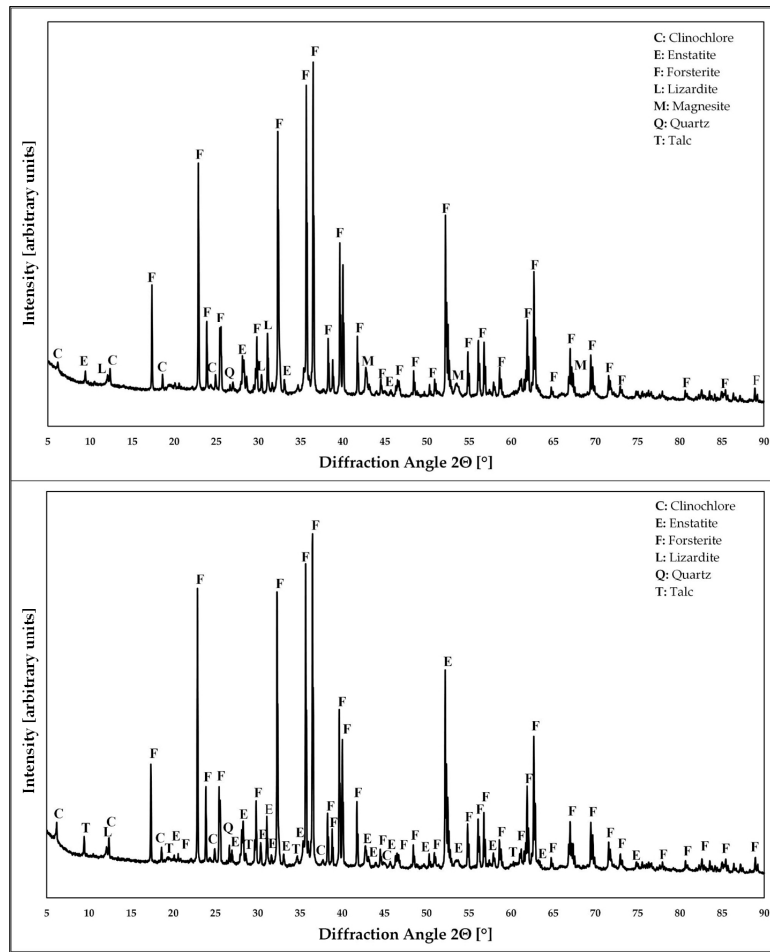


**Figure 4.** XRD pattern of carbonation product fraction 11–20 μm before (top) and after (bottom) deagglomeration by attrition.

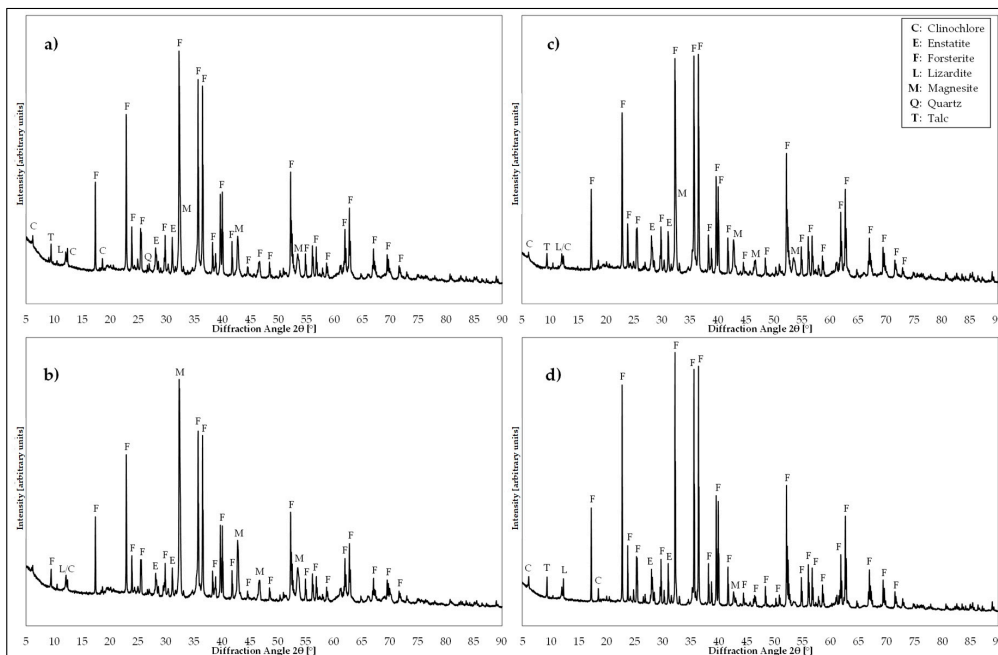


**Figure 5.** Carbonation product of olivine <20 μm, separation by attrition and sieving, (a) carbonation product prior to separation, (b) fraction 0–5 μm, (c) fraction 5–11 μm, (d) fraction 11–15 μm.

**Table 4.** Semiquantitative determination (XRD pattern of Figure 5) and yield (in grey) of the olivine (<20 µm) carbonation product and different product fractions after classification.

Mineral Phase Fraction [%]	Carbonation Product 0–20 µm	0–5 µm	5–11 µm	11–15 µm
Mass fraction	100 *	~45	~40	~12
Forsterite	50–55	45–50	65–70	70–75
Magnesite	20–25	30–35	10–15	5–10
Enstatite	10–15	5–10	10–15	10–15
Clinochlore	5–10	≤5	≤5	≤5
Talc	≤5	≤5	≤5	≤5
Lizardite	≤5	≤5	≤5	≤5
Quartz	≤5	≤5	≤5	≤5

\* 3% of total mass belongs to fraction 15–20 µm.

The XRD patterns for the deagglomeration and classification of the ferrochrome slag can be seen in Figure 6. All listed different particle size fractions show a high peak and some smaller peaks for calcite. In the initial carbonation product of the investigated ferrochrome slag <63 µm (Figure 6a), also clinochlore, aragonite, enstatite and merwinite are visible. The pattern of fraction 0–5 µm (Figure 6b), which is identical to the pattern for fraction 5–11 µm, only shows peaks for calcite and a short peak for chromium oxalate hydrate, which is a result of the oxalic acid as an additive in the carbonation process and its accumulation in the fine particle size fractions.

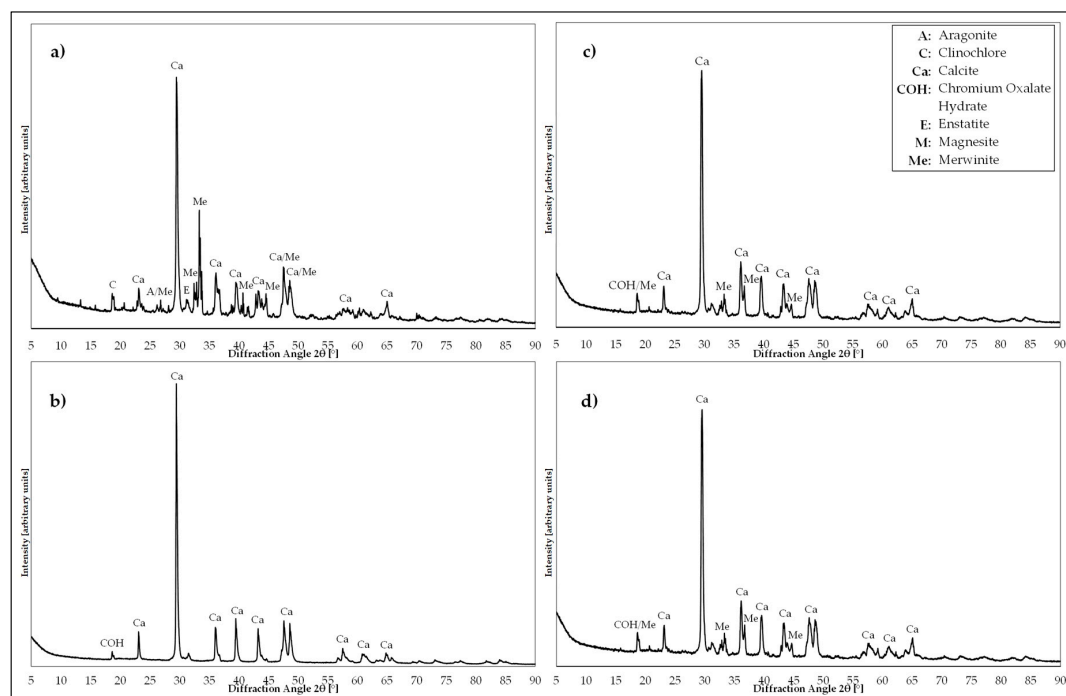
**Figure 6.** Carbonation product of Ferrochrome Slag <63 µm, separation by attrition and sieving—(a) carbonation product prior to separation, (b) fraction 0–5 µm, (c) fraction 11–15 µm, (d) fraction 15–20 µm.

Table 5 shows the semiquantitative determination of the contained mineral phases for the different particle size fractions of the carbonated ferrochrome slag. All fractions below 20 µm, which together make up a mass of 53%, show good results for the enrichment of magnesite.

**Table 5.** Semiquantitative determination (XRD pattern of Figure 6) of the ferrochrome slag (<63 µm) carbonation product and different product fractions after classification.

Mineral Phase Fraction [%]	Carbonation Product 0–63 µm	0–5 µm	5–11 µm	11–15 µm	15–20 µm
Mass Fraction	100 *	~10	~25	~10	~8
Calcite	50–55	100 **	100 **	95–100	75–80
Merwinite	15–20			5–10	20–25
Magnesite	5–10				
Aragonite	≤5				
Clinocllore	10–15	below detection limit (bdl)	bdl	bdl	bdl
Forsterite	5–10				
Enstatite	≤5				
Quartz	≤5				

\* 47% of total mass belongs to fraction 20–63 µm, \*\* XRF show 20–22% SiO<sub>2</sub>, which is supposed to be amorphous as it is not visible in the XRD pattern.

The XRD results of the fraction 0–11 µm with a purity of nearly 100%—not considering the phases below the detection limit—show a recovery of 66.5% at a yield of 35%. Combining these XRD results with XRF measurements for this carbonation product show a SiO<sub>2</sub> content of ~21%. As silicon dioxide is not contained in calcite it can be assumed that it is available as amorphous silica in this product.

#### 4. Discussion

Regarding the main objective of the CO<sub>2</sub>MIN project to use mineral sequestration of carbon dioxide for long-term storage of anthropogenic CO<sub>2</sub>, with a focus on generating replacement material for the cement industry, continuous progress was made. For primary feedstock material, namely olivine, a carbonation degree of up to 23% and for the secondary material, the ferrochrome slag, a carbonation degree of 46% was achieved, which represented a CO<sub>2</sub> uptake of 116.5 kg<sub>CO<sub>2</sub></sub>/t<sub>feed</sub> for olivine and 218.5 kg<sub>CO<sub>2</sub></sub>/t<sub>feed</sub> for the ferrochrome slag, respectively. The carbonation degree was related to the reactive components of magnesium, calcium and iron.

The separation of single products, artificial mixtures and specific processing steps works in specific conditions. However, the full separation of the three phases—unreacted material, magnesite/calcite and amorphous silica—could not be obtained by now. The grinding process has a significant influence on further separation and metallurgical treatment [33–36]. The effect of different aggregates for comminution in lab-scale tests and scale-up carbonation test work, e.g., dry fine grinding with high pressure grinding roll or vertical roller mill, will be part of future investigations. The liberation of the phases has to be improved and some separation methods are facing their limits due to the very small particle size of the phases to be separated.

The separation tests for attrition and classification as well as for flotation showed promising results, regarding the separation of magnesite or calcite from unreacted feed material. A recovery of ~65% of the carbonate was achieved for the fine particle size fraction via classification and even 72% by flotation. The purity of the carbonated fine olivine product 0–5 µm with 30–35 µm magnesite is still low, which is a result of the carbonation degree of only 23%. The high amount (~50%) of initial olivine material below 5 µm that did not react during the carbonation process, resulted in fine unreacted olivine, which stays in the fine fraction after the classification process. To achieve better results, the carbonation degree needs to be improved but also the reason for the limited reaction of the finely ground olivine must be further investigated.

The purity of the fine carbonated slag product is very high, due to higher initial particle size and higher reactivity of the initial material. The carbonation degree is much higher at 46%.

However, the SEM images of coarser particle size fractions for both olivine and ferrochrome slag after carbonation still show amorphous silica and magnesite on the surface of the unreacted material. Therefore, the deagglomeration needs improvement to increase the recovery of the reaction products

and to decrease the recirculating mass of those products back into the carbonation process with the unreacted material.

A further step for the separation of the amorphous silica from the magnesite could be ultrafine classification at 1  $\mu\text{m}$ , which is part of the future work and also the usage of hydrocyclones and classification centrifuges for higher throughput. A combination of the single separation processes will be performed to obtain an enriched product, which can be used as a substitute in the cement industry and application tests for the separation products will be performed.

**Author Contributions:** Conceptualization, D.K.; methodology, D.K.; investigation, D.K.; validation, H.W.; writing—original draft preparation, D.K.; writing—review and editing, H.W.; visualization, D.K.; supervision, H.W.; All authors have read and agreed to the published version of the manuscript.

**Funding:** The authors are grateful for the financial support within the CO2MIN project which was funded by BMBF (Federal Ministry of Education and Research), project number: 033RCO14B.

**Acknowledgments:** For the continuous support and cooperation, we would like to thank our project partners Simon Etzold, GHI, for the analyses; Srecko Stopic and Christian Dertmann, IME, for the carbonation tests; Andreas Bremen, AVT-SVT, Hesam Ostovari, LTT, (all RWTH Aachen), as well as Till Strunge, IASS Potsdam, Pol Knops, Green Minerals and Peter Blaum and Jan Skocek from HeidelbergCement.

**Conflicts of Interest:** The authors declare no conflict of interest.

## References

1. Rebecca Lindsey. Climate Change: Atmospheric Carbon Dioxide. Available online: <https://www.climate.gov/news-features/understanding-climate/climate-change-atmospheric-carbon-dioxide> (accessed on 5 November 2020).
2. Blunden, J.; Arndt, D.S. State of the Climate in 2018. *Bull. Amer. Meteor. Soc.* **2019**, *100*, Si–S306. [CrossRef]
3. Kelemen, P.; Benson, S.M.; Pilorgé, H.; Psarras, P.; Wilcox, J. An Overview of the Status and Challenges of CO<sub>2</sub> Storage in Minerals and Geological Formations. *Front. Clim.* **2019**, *1*, 297. [CrossRef]
4. Huijgen, W.J.J. *Carbon Dioxide Sequestration by Mineral Carbonation*; Energy research Centre of the Netherlands (ECN): Petten, The Netherlands, 2007; ISBN 90-8504-573-8.
5. Pan, S.-Y.; Chiang, A.; Chang, E.-E.; Lin, Y.-P.; Kim, H.; Chiang, P.-C. An Innovative Approach to Integrated Carbon Mineralization and Waste Utilization: A Review. *Aerosol Air Qual. Res.* **2015**, *15*, 1072–1091. [CrossRef]
6. Ostovari, H.; Sternberg, A.; Bardow, A. Rock ‘n’ use of CO<sub>2</sub>: Carbon footprint of carbon capture and utilization by mineralization. *Sustain. Energy Fuels* **2020**, *4*, 4482–4496. [CrossRef]
7. Kremer, D.; Etzold, S.; Boldt, J.; Blaum, P.; Hahn, K.M.; Wotruba, H.; Telle, R. Geological Mapping and Characterization of Possible Primary Input Materials for the Mineral Sequestration of Carbon Dioxide in Europe. *Minerals* **2019**, *9*, 485. [CrossRef]
8. Bremen, A.M.; Ploch, T.; Mhamdi, A.; Mitsos, A. A mechanistic model of direct forsterite carbonation. *Chem. Eng. J.* **2021**, *404*, 126480. [CrossRef]
9. Baris, K.; Ozarslan, A.; Sahin, N. The Assessment for CO<sub>2</sub> Sequestration Potential by Magnesium silicate Minerals in Turkey: Cases of Orhaneli-Bursa and Divrigi-Sivas Regions. *Energy Explor. Exploit.* **2008**, *26*, 293–309. [CrossRef]
10. Daval, D. Carbon dioxide sequestration through silicate degradation and carbon mineralisation: Promises and uncertainties. *NPJ Mater. Degrad.* **2018**, *2*, 1677. [CrossRef]
11. Andrew, R.M. *Global CO<sub>2</sub> Emissions from Cement Production, 1928–2018*; Earth System Science Data; Copernicus: Göttingen, Germany, 2019; Volume 11, pp. 1675–1710. [CrossRef]
12. Gibbs, M.J.; Soyka, P.; Conneely, D. *CO<sub>2</sub> Emissions from Cement Production. Good Practice Guidance and Uncertainty Management in National Greenhouse Gas Inventories*; Intergovernmental Panel on Climate Change (ipcc): Geneva, Switzerland, 2000; Available online: [https://www.ipcc-nggip.iges.or.jp/public/gp/bgp/3\\_1\\_Cement\\_Production.pdf](https://www.ipcc-nggip.iges.or.jp/public/gp/bgp/3_1_Cement_Production.pdf) (accessed on 10 November 2020).
13. Sanna, A.; Uibu, M.; Caramanna, G.; Kuusik, R.; Maroto-Valer, M.M. A review of mineral carbonation technologies to sequester CO<sub>2</sub>. *Chem. Soc. Rev.* **2014**, *43*, 8049–8080. [CrossRef]
14. Rotheron, R.; Paynter, C. Calcium Carbonate Fillers. In *Fillers for Polymer Applications*; Rotheron, R., Ed.; Springer International Publishing: Cham, Switzerland, 2017; pp. 149–160. ISBN 978-3-319-28116-2.

15. Khan, I.; Bhat, A.H. CHAPTER 16. Micro and Nano Calcium Carbonate Filled Natural Rubber Composites and Nanocomposites. In *Natural Rubber Materials*; Thomas, S., Han Chan, C., Pothen, L., Joy, J., Maria, H., Eds.; Royal Society of Chemistry: Cambridge, UK, 2013; pp. 467–487. ISBN 978-1-84973-631-2.
16. Min, Y.; Jun, Y.-S. Wollastonite carbonation in water-bearing supercritical CO<sub>2</sub>: Effects of water saturation conditions, temperature, and pressure. *Chem. Geol.* **2018**, *483*, 239–246. [[CrossRef](#)]
17. Huijgen, W.J.; Witkamp, G.-J.; Comans, R.N. Mechanisms of aqueous wollastonite carbonation as a possible CO<sub>2</sub> sequestration process. *Chem. Eng. Sci.* **2006**, *61*, 4242–4251. [[CrossRef](#)]
18. Ryu, K.W.; Jo, H.; Choi, S.H.; Chae, S.C.; Jang, Y.-N. Changes in mineral assemblages during serpentine carbonation. *Appl. Clay Sci.* **2016**, *134*, 62–67. [[CrossRef](#)]
19. Blencoe, J.G.; Anovitz, L.M.; Beard, J.S.; Palmer, D.A. *Carbonation of Serpentine for Long-Term CO<sub>2</sub> Sequestration*; Final Report; FY 2003 ORNL Laboratory Directed Research and Development Annual Report Project Number: 3210-2024; Oak Ridge National Laboratory: Oak Ridge, TN, USA, 2003.
20. Okrusch, M.; Matthes, S. *Mineralogie*; Springer: Berlin/Heidelberg, Germany, 2014; ISBN 978-3-642-34659-0.
21. O'Driscoll, M. Olivine-Going where the grass is greener. *Ind. Miner.* **2004**, *438*, 40–49.
22. Boyd, R.; Gautneb, H. *Mineral Resources in Norway: Potential and Strategic Importance, 2016 Update*; Geological Survey of Norway: Trondheim, Norway, 2016; Available online: <https://www.researchgate.net/publication/309807416> (accessed on 23 January 2020).
23. Stopic, S.; Dertmann, C.; Modolo, G.; Kegler, P.; Neumeier, S.; Kremer, D.; Wotruba, H.; Etzold, S.; Telle, R.; Rosani, D.; et al. Synthesis of Magnesium Carbonate via Carbonation under High Pressure in an Autoclave. *Metals* **2018**, *8*, 993. [[CrossRef](#)]
24. Stopic, S.; Dertmann, C.; Koiwa, I.; Kremer, D.; Wotruba, H.; Etzold, S.; Telle, R.; Knops, P.; Friedrich, B. Synthesis of Nanosilica via Olivine Mineral Carbonation under High Pressure in an Autoclave. *Metals* **2019**, *9*, 708. [[CrossRef](#)]
25. Béarat, H.; McKelvy, M.J.; Chizmeshya, A.V.G.; Gormley, D.; Nunez, R.; Carpenter, R.W.; Squires, K.; Wolf, G.H. Carbon sequestration via aqueous olivine mineral carbonation: Role of passivating layer formation. *Environ. Sci. Technol.* **2006**, *40*, 4802–4808. [[CrossRef](#)]
26. Eikeland, E.; Blichfeld, A.B.; Tyrsted, C.; Jensen, A.; Iversen, B.B. Optimized carbonation of magnesium silicate mineral for CO<sub>2</sub> storage. *ACS Appl. Mater. Interfaces* **2015**, *7*, 5258–5264. [[CrossRef](#)]
27. Lazaro, A.; Brouwers, H.; Quercia, G.; Geus, J.W. The properties of amorphous nano-silica synthesized by the dissolution of olivine. *Chem. Eng. J.* **2012**, *211–212*, 112–121. [[CrossRef](#)]
28. Raza, N.; Raza, W.; Madeddu, S.; Agbe, H.; Kumar, R.V.; Kim, K.-H. Synthesis and characterization of amorphous precipitated silica from alkaline dissolution of olivine. *RSC Adv.* **2018**, *8*, 32651–32658. [[CrossRef](#)]
29. Matus, C.; Stopic, S.; Etzold, S.; Kremer, D.; Wotruba, H.; Dertmann, C.; Telle, R.; Friedrich, B.; Knops, P. Mechanism of Nickel, Magnesium, and Iron Recovery from Olivine Bearing Ore during Leaching with Hydrochloric Acid Including a Carbonation Pre-Treatment. *Metals* **2020**, *10*, 811. [[CrossRef](#)]
30. O'Connor, W.K.; Dahlin, D.C.; Dahlin, C.L.; Collins, W.K. Carbon Dioxide Sequestration by Direct Mineral Carbonation: Process Mineralogy of Feed and Products: 2001. In Proceedings of the 2001 SME Annual Meeting & Exhibit, Denver, CO, USA, 26–28 February 2001; Society for Mining, Metallurgy, and Exploration: Littleton, CO, USA, 2001.
31. Ding, K.; Laskowski, J.S. Application of a modified water glass in a cationic flotation of calcite and dolomite. *Can. Metall. Q.* **2013**, *45*, 199–206. [[CrossRef](#)]
32. Yao, J.; Hou, Y.; Wang, Y.L.; Zhong, W.X.; Yin, W.Z. Research on the Floatability of Magnesite and its Gangue Minerals with Sodium Oleate and Lauryl Amine as Collectors. *AMR* **2013**, *798–799*, 328–332. [[CrossRef](#)]
33. Katzmarzyk, J.L.; Silin, I.; Hahn, K.M.; Wotruba, H.; Gerold, C.; Stapelmann, M. Investigation on flotation behavior of a copper sulfide ore after grinding by Loesche vertical roller mill: Project: Flotation of sulphides after dry comminution. In Proceedings of the 58th Annual Conference of Metallurgists (COM 2019), Vancouver, BC, Canada, 18–21 August 2019; The Metallurgy and Materials Society (MetSoc): Westmount, QC, Canada, 2019.
34. Achimovičová, M.; Vonderstein, C.; Friedrich, B. *Titanium Dioxide. Mechanically Activated Rutile and Ilmenite as the Starting Materials for Process of Titanium Alloys Production*; InTechOpen: London, UK, 2017. [[CrossRef](#)]

35. Schosseler, J.; Trentmann, A.; Friedrich, B.; Hahn, K.; Wotruba, H. Kinetic Investigation of Silver Recycling by Leaching from Mechanical Pre-Treated Oxygen-Depolarized Cathodes Containing PTFE and Nickel. *Metals* **2019**, *9*, 187. [[CrossRef](#)]
36. Silin, I.; Huben, J.; Wotruba, H.; Ognyanova, A. Study on the Characterisation and Processing of Iron Ore after Grinding by HPGR. In Proceedings of the 29th International Mineral Processing Congress (IMPC 2018), Moscow, Russia, 17–21 September 2018; “Ore and Metals” Publishing house: Moscow, Russia; pp. 17–21.

**Publisher’s Note:** MDPI stays neutral with regard to jurisdictional claims in published maps and institutional affiliations.



© 2020 by the authors. Licensee MDPI, Basel, Switzerland. This article is an open access article distributed under the terms and conditions of the Creative Commons Attribution (CC BY) license (<http://creativecommons.org/licenses/by/4.0/>).